CROATICA CHEMICA ACTA
CCACAA **80** (3-4) 421–428 (2007)

ISSN-0011-1643
CCA-3184
Original Scientific Paper

Microscopic Protonation Mechanism of Branched Polyamines: Poly(amidoamine) *versus* Poly(propyleneimine) Dendrimers*

Duško Čakara[a,] and Michal Borkovec[b]**

[a]*Laboratory of Physical Chemistry, Department of Chemistry, Faculty of Science, University of Zagreb, Horvatovac 102 A, HR-10000, Zagreb, Croatia*

[b]*Department of Inorganic, Analytical, and Applied Chemistry, University of Geneva, Quai Ernest-Ansermet 30, 1211 Geneva 4, Switzerland*

RECEIVED FEBRUARY 22, 2007; REVISED MAY 8, 2007; ACCEPTED MAY 9, 2007

Keywords
dendrimer
polyamine
protonation
mechanism
PAMAM
PPI
hyperbranched
polyelectrolyte
gene vector
transfection

The protonation mechanisms of the poly(amidoamine) (PAMAM) andpoly(propyleneimine) (PPI) dendrimers are clarified and related to their molecular structure. The overall proton binding isotherms can be interpreted in terms of a site binding model, which involves a limited number of parameters, and can be used to gain detailed insight in both macroscopic and microscopic protonation mechanisms. The protonation of the PAMAM dendrimers is dominated by the chemical environment of the amine sites, and the sites protonate almost independently leading to protonation mechanism with a characteristic intermediate core-shell structure. In the case of PPI, the protonation is dominated by the electrostatic nearest-neighbor repulsions between the protonated sites, and leads to an intermediate »onion-like« structure where all the odd shells are protonated.

INTRODUCTION

More than two decades after their discovery, dendrimers continue to fascinate the scientific community.[1–3] The most commonly studied ones are the poly(amidoamine) (PAMAM) and the poly(propyleneimine) (PPI) dendrimers (see Figure 1). The PAMAM dendrimers feature a short core chain with two carbon atoms and long amidoamine arms. In the case of PPI dendrimer, the core chain consists of four carbon atoms, while the arms are shorter and contains only three carbon atoms. The zeroth generation dendrimers consist of two tertiary amine groups in the core, and four peripheric primary amine groups, while the higher generations are obtained by adding two chains to each primary amine group in a shell-wise manner (*cf*. Figure 1). The unique properties of these polyamines are related to the regular hyperbranched structure, the well-defined size in the nanometer range, and a very large number of reactive sites that can be functionalized. Dendrimers were proposed in the context of many applications, such as catalysts, chelators, drug carriers, or gene vectors.[3–9]

The physical properties of dendrimers, such as their molecular conformation, intrinsic viscosity, adsorption affinity, depend on the molecular charge, which in turn is determined by the protonation state of the dendrimer. This point leads us to the main question of the protonation mechanism of such dendrimers, which is treated in this contribution in detail. Furthermore, one would like

* Dedicated to Professor Nikola Kallay on the occasion of his 65th birthday.

** Author to whom correspondence should be addressed. (E-mail: dcakara@chem.pmf.hr)

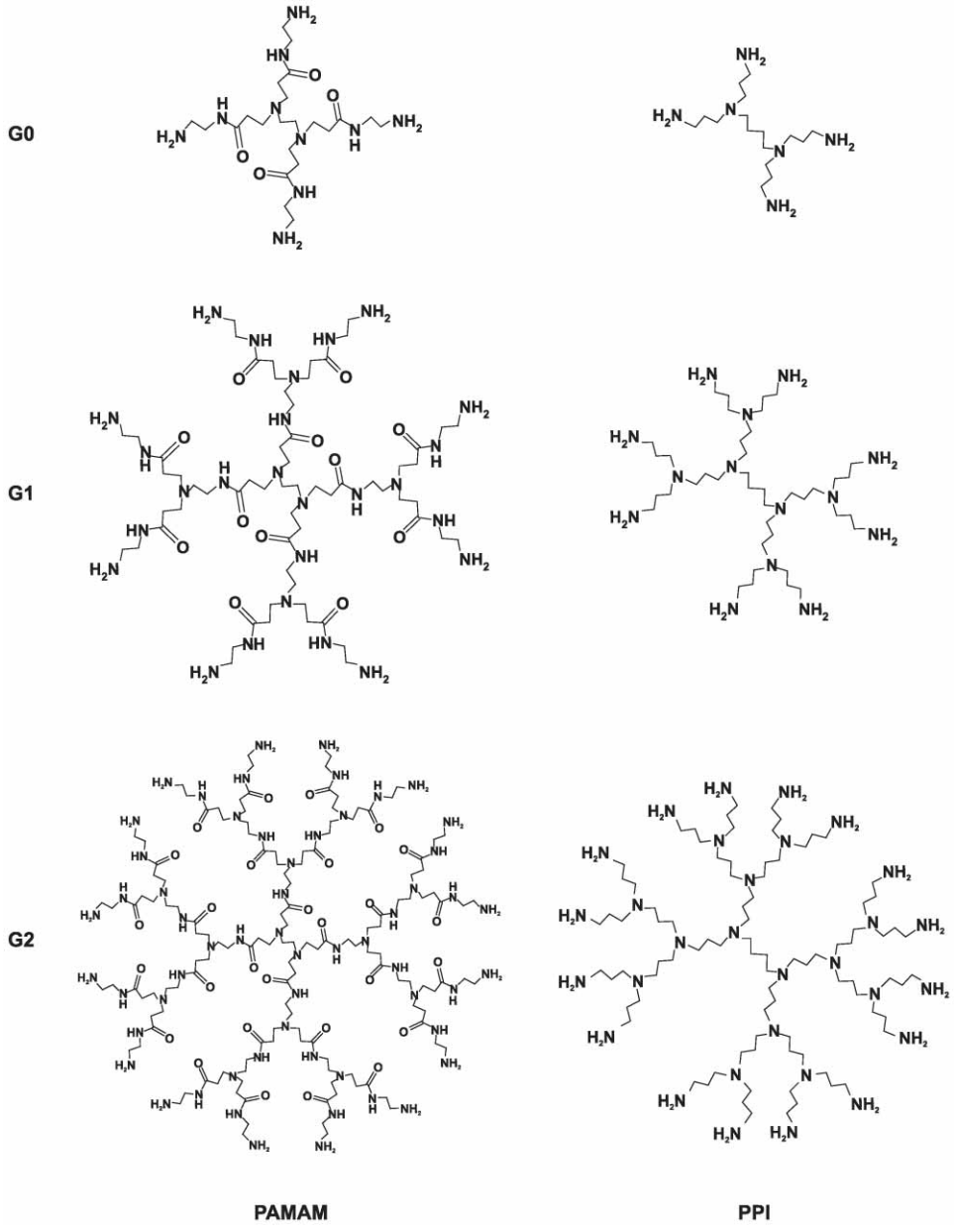

Figure 1. Molecular structure of the first three generations of PAMAM and PPI dendrimers.

to understand the differences in the protonation mechanisms between the PAPAM and PPI dendrimers, related to their different molecular structures.

The protonation behavior of PAMAM and PPI dendrimers was studied by potentiometric acid-base titrations[10,11] and by nuclear magnetic resonance (NMR).[12] The NMR data give microscopic information on the protonation behavior, but they require costly experiments in highly concentrated solutions and give results of limited accuracy. It was shown that basically equivalent microscopic information can be obtained from potentiometric titration data,[10] to which one fits directly the site binding model discussed here. Moreover, this analysis can be carried out in fairly dilute solutions and yields more accurate data. From the model parameters, all the necessary details on the microscopic and macroscopic protonation mechanisms can be obtained.

SITE BINDING MODEL

Consider a polyprotic molecule with N ionizable sites. The macroscopic protonation state, or simply the macrostate, is specified by the number of bound protons m. The microscopic protonation state, or the microstate, is specified by the protonation state of each individual site, in other words the intramolecular distribution of the bound protons. The site binding model described in the following will be used to predict both the microspcopic and

macroscopic protonation states of a dendrimer, depending on the solution pH. Only a moderate number of parameters will be needed for the description.

MICROSCOPIC EQUILIBRIA

The protonation state of a particular amine site i is described by a state variable s_i (i = 1,2,..., N), such that $s_i = 1$ if the site is protonated and $s_i = 0$ if the site is deprotonated. The microstate can be specified by the entire set of state variables $\{s_i\}$. Intermolecular interactions can be neglected in dilute solutions, and the free energy of a given microstate relative to the fully deprotonated state can be written in terms of the so-called Ising Hamiltonian

$$\frac{\beta F(\{s_i\})}{\ln 10} = -\sum_i \mathrm{p}\hat{K}_i s_i + \frac{1}{2!}\sum_{i,j} \varepsilon_{ij} s_i s_j + \ldots \qquad (1)$$

where the indices run over all the sites, $\mathrm{p}\hat{K}_i$ is the microscopic protonation constant of the site i given all other sites are deprotonated, ε_{ij} are pair interaction parameters, and $\beta = 1 / kT$ is the inverse thermal energy.[11–14] The parameters ε_{ij} are related to the dimensionless free energy of the electrostatic repulsion between the protonated sites. The multiplication of ε_{ij} with s_i and s_j in Eq. (1) ensures that only the interactions between the protonated sites are taken into account. As well, the symmetry relation $\varepsilon_{ij} = \varepsilon_{ji}$ is obeyed, and one has $\varepsilon_{ii} = 0$. In the first approximation, we consider only the nearest-neighbor pair interactions and neglect the higher order ones, whereby the present model becomes equivalent to the classical Ising model.[15,16]

The parameters $\mathrm{p}\hat{K}_i$ and ε_{ij} are also called the *cluster parameters*.[17] The number of independent parameters can be reduced, since same $\mathrm{p}\hat{K}_i$ values can be assigned to sites with the same chemical environment, and the ε_{ij} values become negligible for distant sites, and have to be only considered between nearest neighbors. The latter strongly depend on the distance between the sites.[18] Thus, even molecules with large number of protonation sites can be described with a moderate set of parameters.

Once the cluster parameters are determined, the model defined through Eq. (1) allows us to calculate all the quantities related to both macroscopic and the microscopic equilibria as a function of pH. The probability, or the mole fraction, of a given microstate depends on the proton activity, a_H, and can be expressed as:[13,14]

$$p(\{s_i\}) = \Xi^{-1} a_H^m e^{-\beta F(\{s_i\})} \qquad (2)$$

The normalization constant Ξ can be interpreted as the partition function of the polyelectrolyte:

$$\Xi = \sum_{\{s_i\}} a_\mathrm{H}^m e^{-\beta F(\{s_i\})} \qquad (3)$$

where the fully unprotonated molecule is taken as the reference state. The probability of a microstate, can be expressed as the following product

$$p(\{s_i\}) = \pi(\{s_i\}) P_m(a_\mathrm{H}) \qquad (4)$$

where $P_m(a_\mathrm{H})$ denotes the pH-dependent probability of a macrostate, and $\pi(\{s_i\})$ is the conditional probability of the microstate $\{s_i\}$ within the macrostate m. This probability is given by

$$\pi(\{s_i\}) = \overline{K}_m^{-1} e^{-\beta F(\{s_i\})} \qquad (5)$$

where $\overline{K}_m$ denotes the so-called cumulative constants (see the following section). The important consequence of Eq. (4) is that the probability $\pi(\{s_i\})$ does not depend on pH, and can be easily interpreted as the mole fraction of the microspecies within a macrospecies m.

If the unprotonated site is labelled with j, the association equilibrium can be written as

$$\mathrm{A}\{s_i\} + \mathrm{H} \rightleftharpoons \mathrm{A}\{s'_i\} \qquad (6)$$

where $s_i = s'_i$ for all $i \neq j$, but $s_j = 0$ and $s'_j = 1$. With the expansion for the free energy Eq. (1), the microscopic pK value for the reaction given by Eq. (6) can be expressed as[19]

$$\mathrm{p}\hat{K}_{i,\{s_i\}} = \mathrm{p}\hat{K}_i - \sum_j \varepsilon_{ij} s_j - \ldots \qquad (7)$$

This relation defines the change in the microscopic protonation constant of site i, in the presence of other protonated sites, and reflects the group additivity concept for the estimation of protonation constants.[20] The microconstants from Eq. (7) represent secondary quantities, which can be easily evaluated once the primary cluster parameters are known. Note that the microconstants $\mathrm{p}\hat{K}_i$ entering the cluster parameters is a specific case of $\mathrm{p}\hat{K}_{i,\{s_i\}}$ for $s_i = 0$ for all i = 1,..., N.

MACROSCOPIC EQUILIBRIA

The classical macroscopic description of protonation equilibria assigns a macroscopic protonation constant to each protonation step:

$$K_m = \frac{[H_m A]}{[H_{(m-1)} A] a_\mathrm{H}} \qquad (8)$$

These constants are referred to as step-wise constants, while the so-called cumulative constants are defined as:

$$\overline{K}_m = \prod_{i=1}^{m} K_i \qquad (9)$$

The latter can be related to the free energy introduced above:[19]

$$\overline{K}_m = \sum_{\{s_i\}} e^{-\beta F(\{s_i\})} \delta_{m,\sum_j s_j} \tag{10}$$

where δ_{ij} is Kronecker symbol, and δ_{ii} =1 and vanishes otherwise. The commonly used macroscopic step-wise dissociation constants (Eq. (8)) can be expressed in terms of the cumulative constants as $pK_m = \log_{10} K_m = \log_{10} (\overline{K}_m / \overline{K}_{m-1})$.

The probabilities of the macrostates, P_m, are related to the proton activity and the cumulative constants through:

$$P_m(a_H) = \Xi^{-1} \overline{K}_m a_H^m \tag{11}$$

where the normalization constant is the aforementioned partition function (*cf.* Eq. (3)), which can be also written as the so called *binding polynomial*[13]

$$\Xi = \sum_{n=0}^{N} \overline{K}_m a_H^n \tag{12}$$

The degree of protonation, θ, can be calculated from the probabilities of the macrostates P_m as

$$\theta = \frac{1}{N} \sum_{m=1}^{N} m P_m \tag{13}$$

or alternatively expressed as

$$\theta = \frac{a_H}{N} \frac{\partial \log \Xi}{\partial a_H} \tag{14}$$

The cluster parameters are determined by least-squares fitting of experimental titration curved with the degree of protonation Eq. (14).

MICROSCOPIC PROTONATION MECHANISM

Once the cluster parameters $p\hat{K}_i$ and ε_{ij} are known, the microscopic speciation diagrams can be determined. The schemes used for the dendrimers are represented in Figure 2.

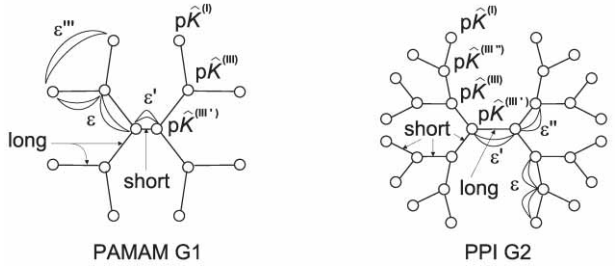

Figure 2. Schematic representation of PAMAM and PPI dendrimers with the assignment of the cluster parameters.

TABLE I. Cluster parameters for the PPI dendrimers at an ionic strength 0.1 mol dm^{-3} [11]

generation	$pK^{(I)}$	$pK^{(III)}$	$pK^{(III')}$	$pK^{(III'')}$	ε''	ε'	ε
0	9.97	–	9.02	–	1.05	0.61	–
1	9.85	–	8.19	9.66	1.05	0.61	1.57
2	9.79	7.99	8.19	9.72	1.05	0.61	1.57
3	9.70	8.02	8.19	9.71	1.05	0.61	1.57
4	9.56	7.95	8.19	9.66	1.05	0.61	1.57

TABLE II. Cluster parameters for the PAMAM dendrimers at an ionic strength 0.1 mol dm^{-3}.[10] The next-nearest neighbor parameter ε''' is given by the value of Δ by Eq. (15)

$pK^{(I)}$	$pK^{(III)}$	$pK^{(III')}$	ε	ε'	Δ
9.00	6.00	6.70	0.15	2.85	0.14

The microconstants of the primary amine groups are denoted with $p\hat{K}^{(I)}$. Among the tertiary groups, we distinguish the core tertiary groups, which are assigned with $p\hat{K}^{(III')}$, and in the case of PPI, we further distinguish the outermost shell tertiary groups, assigned with $p\hat{K}^{(III'')}$. The rest of the tertiary groups are assigned with $p\hat{K}^{(III)}$.

The pair interaction parameters between the sites on the dendrimer arms are denoted by ε, while between the two innermost sites by ε'. The parameter ε'' specifies the interaction between the intermost site and the next outer site in the PPI dendrimer. The parameter ε''' denotes the interaction between the neighboring outermost primary amine groups in the PAMAM dendrimer. This interaction is negligible in the PPI case.

In the case of PPI dendrimers, van Duijvenbode *et al.*[11] have fitted the experimental titration curves to the site binding model and obtained the values summarized in Table I. One observes that the $p\hat{K}^{(I)}$ and $p\hat{K}^{(III'')}$ are somewhat higher than the rest, indicating that the corresponding sites are somewhat more basic. The pK values decrease with increasing generation number, indicating that all groups become more acidic in the larger dendrimers. On the other hand, pair interaction parameters are independent of the generation number. Note that these interactions are important between all groups on the dendrimer arms, while being quite insignificant for the two central groups.

In the case of PAMAM dendrimers, the experimental proton binding isotherms for generation 0 through 6 could be fitted with six parameters only (*cf.* Table II).[10] The characteristic feature is that the primary amine groups are significantly more basic than the tertiary amine groups, while the two innermost tertiary groups are slightly more basic. In contrast to the PPI case, the interaction parameters are very small, except for the two in-

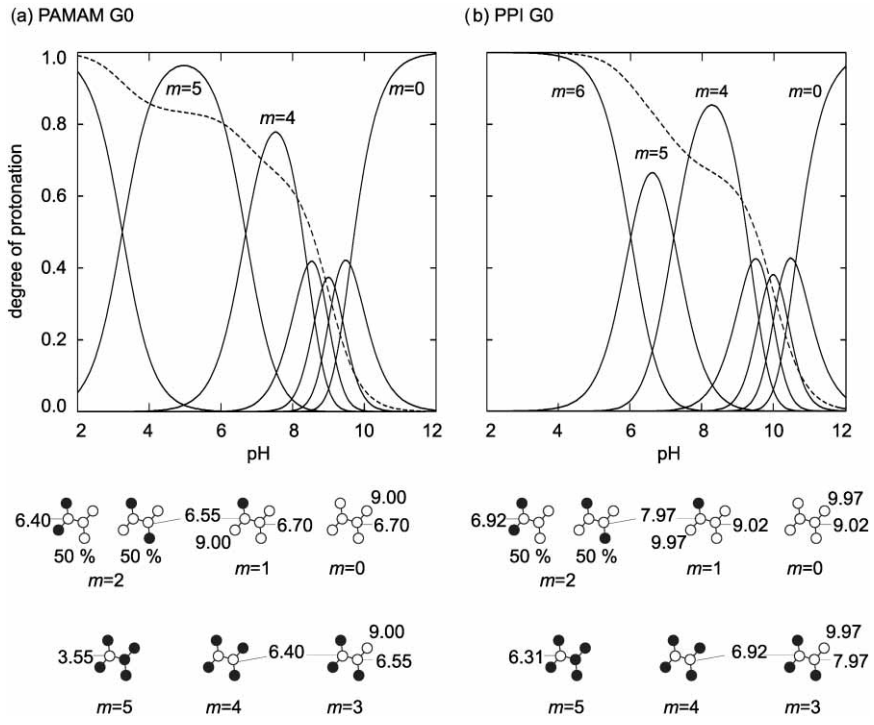

Figure 3. Speciation diagrams for the G0 PAMAM (a) and PPI (b) dendrimers at 0.1 mol dm^{-3} ionic strength. The full lines describe the macroscopic speciation, while the dashed curve is the overall proton binding isotherm. The protonation microspecies, and the microconstants for each unprotonated site are given in the lower part of the figure.

nermost groups. Note that with exception of the next-nearest neighbor interaction between the primary amines ε''', the cluster parameters for the PAMAM dendrimer do not vary with the generation number. The ε''' can be estimated for each generation number k from the empirical relationship:

$$\varepsilon''' = \Delta\,(k–1) \qquad (15)$$

where $\Delta = 0.14$ and $k = 2,..., 6$ denotes the generation number. For $k = 0$, 1 $\varepsilon''' = 0$. Relation 15 applies only for lower generations, for higher generations we estimate somewhat larger ε''' values in the order of ≃1.

The protonation mechanism is obtained by calculating the protonation free energy and the corresponding microspecies probabilities with the above described model and the known cluster parameters. Then, the macroscopic speciation is obtained by adding up the microspecies probabilities, and classifying them according to the total number of the protonated sites m.

The speciation diagrams for generation zero of both dendrimers are presented in Figure 3. The macrostate probabilities are represented as a function of pH. The dashed line is the overall macroscopic proton binding isotherm, which reflects the weighted sum of the macrospecies probabilities.

In the case of PAMAM, the overall isotherm exhibits three distinct protonation steps. Roughly, the primary amine groups protonate in the first step at pH ≈ 9.0, while the tertiary amine groups protonate in two well-separated steps at pH ≈ 6.4 and pH ≈ 3.5. In the case of PPI, the primary amine groups protonate near pH ≈ 10.0, while the two inner groups protonate in a single step, between pH ≈ 5.0 and pH ≈ 7.5. The microspecies are similar for both types of dendrimers, as presented in the lower part of Figure 3. The microstates corresponding to each macrostate are shown, together with the microstate probabilities (in %). With exception of the $m = 2$ macrostate, for which two microstates are present with an equal probability, we observe that only one microstate dominates each macrostate.

The microscopic $p\hat{K}_{i,\{s_i\}}$ values are indicated for each site and each microspecies in the lower part of Figure 3 (*cf.* Eq. (7)). As the pH decreases, the next group to protonate is typically the one with the highest $p\hat{K}_{i,\{s_i\}}$. For both dendrimers, the protonation of the primary amine sites occurs around $p\hat{K}^{(I)}$. In this step, the probability to protonate the tertiary amine protonation remains small. For PAMAM, this effect is due to the significantly lower $p\hat{K}^{(III)}$ than $p\hat{K}^{(I)}$. In the case of PPI, it is a consequence of a high ε value, since $p\hat{K}^{(III)}$ is only moderately lower than $p\hat{K}^{(I)}$. The protonation of the first inner site occurs around pH ≈ 6.5 for both dendrimers. For the second core site to protonate, a three-fold electrostatic repulsion has to be overcome. This effect is significant for PAMAM, while almost negligible for PPI, which explains the distinct protonation step in the case of PAMAM at pH ≈ 3.5.

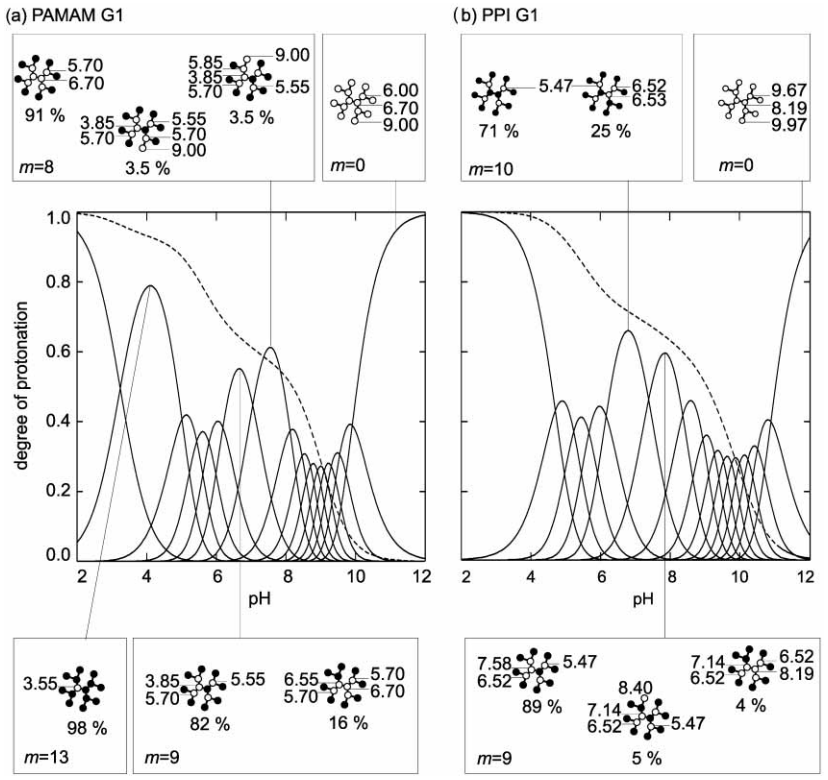

Figure 4. Speciation diagrams for the G1 PAMAM (a) and PPI (b) dendrimers at an ionic strength of 0.1 mol dm^{-3}. The full lines describe the macroscopic speciation, while the dashed curve is the overall proton binding isotherm. The schemes represent the protonation microspeciation for the most significant macrospecies, where the probabilities are indicated for each microstate. The additivity principle (*cf.* Eq. (7)) is reflected in the microscopic protonation constants of the unprotonated sites.

The corresponding step for PPI occurs together with the one near pH ≈ 6.5.

The above consideration can be readily extended to higher generations. The speciation diagrams for the first generation PAMAM and PPI dendrimers are presented in Figure 4. Due to the complexity, which rapidly increases with the generation number, we represent only the most dominant macrospecies and within those, only the more significant microspecies. For both dendrimers, the protonation of the primary amine sites occurs again in a single step, around pH ≈ 9.0 for PAMAM and around pH ≈ 10.0 for PPI. In the case of PAMAM, this process results in the formation of a distinct intermediary macrostate m = 8, where all primary amine sites are protonated. The rest of

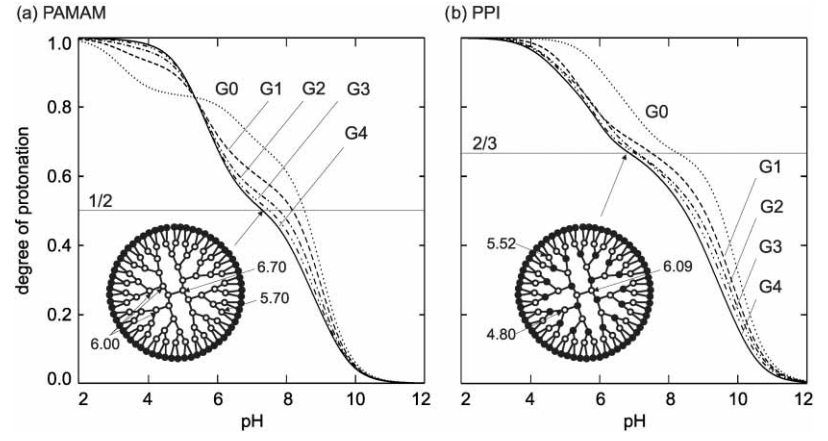

Figure 5. Proton binding isotherms for the first four generation PAMAM (a) and PPI (b) dendrimers at 0.1 mol dm^{-3} ionic strength. The intermediate microspecies (inset) are reminiscent of the protonation mechanisms. The PAMAM dendrimers protonate in a core-shell mechanism, while the PPI protonates in a shell-wise fashion resulting in an »onion-like« intermediate protonation microspecies. The microscopic protonation constants are indicated for each deprotonated shell.

the molecule protonates basically in a single step around pH ≈ 5.9, with exception of the last core site which protonates in a distinguished step near pH ≈ 3.5. This last step is less obvious in the overall titration curve than in the case of G0, because it contributes only with 1/14 to the total degree of protonation, *versus* 1/6 in the case of G0.

In the case of the first generation PPI dendrimer, one core site protonates in the same step as the primary amines, resulting in a distinguished macrostate with $m = 9$. This effect occurs due to the similarity of $p\hat{K}^{(I)}$ and $p\hat{K}^{(III')}$. An additional core tertiary site protonates near pH ≈ 7.58, and we observe an intermediary macrostate with $m = 10$, where the most probable microspecies is the one with the protonated tertiary amine groups in the core and the primary amine sites. The protonation of the remaining four tertiary amines occurs in the second step near pH ≈ 5.5.

The proton binding isotherms for all investigated generations of both dendrimers are presented in Figure 5. In both cases, we observe that with increasing generation number, the curves converge to a common master curve. In this high generation limit, the overall proton binding isotherm for both dendrimers exhibits two distinct steps with an intermediary plateau.

In the case of PAMAM, the primary amine sites protonate in the first step around pH ≈ 8.0, which is followed by a plateau at pH ≈ 7.0. At this plateau, the dominant species has all primary amine groups protonated, as indicated in the inset of Figure 5a. The plateau value of θ reflects the ratio between the primary and the tertiary amine sites of 1/2. The rest of the molecule protonates randomly in the second step around pH ≈ 5.7, with an exception of the second core site, which protonates at pH ≈ 3.6. In the large dendrimer limit, the latter protonation step becomes irrelevant with respect the overall titration curve. It should also be noted that in the case of PAMAM, the next-nearest neighbor repulsion parameter ε''' becomes increasingly important for high generations, causing a broadening of the first protonation step. We conclude that high generation PAMAM dendrimers protonate through a core-shell mechanism, which is due to a substantial difference in the proton affinities of the primary and tertiary sites. The nearest-neighbor electrostatic repulsions play a negligible role.

In the case of PPI, all the sites in odd shells, counting from the outermost, protonate in the first step around pH ≈ 9.0. For high generations, the ratio of the odd shell sites to the total number of sites is 2/3, which explains the higher value of the intermediary plateau. The corresponding dominant microspecies is indicated in the inset of Figure 5b, and is a consequence of relatively high ε values, due to which the protonation of the neighboring sites is avoided. The rest 1/3 sites protonate almost randomly in a second step around pH ≈ 4.5. We conclude that PPI dendrimers protonate in an »onion-like« fashion, where the odd shells protonate at high pH first, and the even shells at lower pH. This behavior is due to the strong repulsive interactions between the amine groups, which have otherwise comparable chemical affinity to protons.

Indeed, the distinct protonation mechanisms of PAMAM and PPI reflect their molecular structures. The mechanism of PAMAM is predominately determined through the different chemical environments of the primary and tertiary amine groups, while the substantial distance between the amine groups along the amidoamine arms of the molecule make their interactions almost negligible. In the case of PPI, the short distances between the amine groups make their interactions important, while the similar affinities to protons of the tertiary and primary groups are due to a similar chemical environment of the two different sites.

The discussed results reflect the ionic strength of 0.1 mol dm^{-3}, but they are illustrative for higher ionic strengths as well. Increasing the ionic strength causes a parallel shift of the protonation steps towards basic pH, but the protonation mechanisms remains unchanged.[10,11] For PAMAM, $p\hat{K}$ values increase with increasing ionic strength, which is typical of weak bases. The nearest-neighbor interaction parameters ε are basically ionic strength independent. On the other hand, in the case of the PPI dendrimers, all parameters were found to depend on the ionic strength.

CONCLUSION

A site binding model has been used to elucidate both the macroscopic and the microscopic protonation mechanisms of PAMAM and PPI dendrimers. The model parameters include microscopic protonation constants for deprotonated molecule, and nearest-neighbor electrostatic repulsion parameters. The main advantage of this description is that the number of these parameters remains moderate even for high generation dendrimers with a large number of ionizable sites.

In the case of PAMAM dendrimers, effects of electrostatic repulsion is negligible, reflecting the large separation of the neighboring sites. The protonation mechanism is dictated by the fact that the primary amine groups have a significantly higher proton affinity than the tertiary amines in the dendrimer interior. As a consequence, PAMAM dendrimers protonate in a core-shell fashion. The protonation of the primary amine group on the shell occurs in the basic pH region, while the tertiary amine groups in the core protonate in a more acidic region. The intermediate protonation microspecies, where the outermost primary amine groups are protonated, occurs in the neutral pH region, and has a degree of protonation of 1/2.

In the case of PPI dendrimers, the protonation mechanism is determined by the strong nearest-neighbor electrostatic repulsions. In the first protonation step, which occurs in the basic pH region, the protonation follows the

principle of nearest neighbor avoidance, resulting in an intermediate onion-like microstate with protonated odd shells, and a degree of protonation of 2/3. The rest of the sites then protonate independently in the acidic pH region.

REFERENCES

1. B. Helms and E. W. Meijer, *Science* **313** (2006) 929–930.
2. M. Ballauff and C. N. Likos, *Angew. Chem., Int. Ed.* **43** (2004) 2998–3020.
3. E. R. Gillies and J. M. J. Fréchet, *Drug Discov. Today* **10** (2005) 35–43.
4. P. Kubát, K. Lang, P. Janda, and P. Anzenbacher Jr., *Langmuir* **21** (2005) 9714–9720.
5. J. R. Baker Jr., X. Shi, and I. J. Majoros, *Mol. Pharmaceutics* **2** (2005) 278–294.
6. V. A. Kabanov, V. G. Sergeyev, O. A. Pyshkina, A. A. Zinchenko, A. B. Zezin, J. G. H. Joosten, J. Brackman, and K. Yoshikawa, *Macromolecules* **33** (2000) 9587–9593.
7. Z. Sideratou, D. Tsiourvas, and C. M. Paleos, *Langmuir* **16** (2000) 1766–1769.
8. Y. Xu and D. Zhao, *Environ. Sci. Technol.* **39** (2005) 2369–2375.
9. R. van Heerbeek, P. C. J. Kamer, P. W. N. M. van Leeuwen, and J. N. H. Reek, *Chem. Rev.* **102** (2002) 3717–3756.
10. D. Čakara, J. Kleimann, and M. Borkovec, *Macromolecules* **36** (2003) 4201–4207.
11. R. C. van Duijvenbode, M. Borkovec, and G. J. M. Koper, *Polymer* **39** (1998) 2657–2664.
12. G. J. M. Koper, M. H. P. van Genderen, C. Elissen-Roman, M. W. P. L. Baars, E. W. Meijer, and M. Borkovec, *J. Am. Chem. Soc.* **119** (1997) 6512–6521.
13. M. Borkovec, B. Jönsson, and G. J. M. Koper, in: E. Matijević (Ed.), *Surf. Colloid Sci.*, Vol. 16., Kluwer Academic/Plenum Publishers, New York, 2001.
14. M. Borkovec and G. J. M. Koper, *Macromolecules* **30** (1997) 2151–2158.
15. A. Katchalsky, J. Mazur, and P. Spitnik, *J. Polymer Sci.* **23** (1957) 513–532.
16. T. L. Hill, *Statistical Thermodynamics*, Dover, New York, 1986.
17. M. Borkovec and G. J. M. Koper, *Anal. Chem.* **72** (2000) 3272–3279.
18. R. C. van Duijvenbode, A. Rajanayagam, G. J. M. Koper, M. Borkovec, W. Paulus, U. Steuerle, and L. Haussling, *Phys. Chem. Chem. Phys.* **24** (1999) 5649–5652.
19. M. Borkovec and G. J. M. Koper, *J. Phys. Chem.* **98** (1994) 6038–6045.
20. D. D. Perrin, B. Dempsey, and E. P. Serjeant, *pKa Prediction for Organic Acids and Bases*, Chapman and Hall, London, 1981.

SAŽETAK

Mikroskopski mehanizmi protonacije razgranatih poliamina: Usporedba poli(amidoamin) i poli(propilenimin) dendrimera

Duško Čakara i Michal Borkovec

Mehanizmi protonacije poli(amidoamin) (PAMAM) i poli(propilenimin) (PPI) dendrimera su razjašnjeni i dovedeni u svezu s molekulskom strukturom. Protonacijske izoterme je moguće interpretirati pomoću modela veznih mjesta, koji uključuje ograničen broj parametara te daje uvid u potankosti kako makroskopskog, tako i mikroskopskog mehanizma protonacije. Protonacija PAMAM dendrimera je pretežno određena kemijskom okolinom amino skupina, koje se protoniraju gotovo neovisno jedna o drugoj. U tom je slučaju za mehanizam karakteristična protonacijska međuvrsta s rasporedom protoniranih mjesta po uzorku jezgra-ljuska. Nasuprot tome, kod PPI dendrimera prevladava elektrostatsko odbijanje neposredno susjednih protoniranih mjesta, što dovodi do međuvrste u kojoj protonirana mjesta zauzimaju neparne ljuske, nalik unutrašnjosti lukovice.